Catalysis Today 158 (2010) 385–392

Contents lists available at ScienceDirect

Catalysis Today

journal homepage: www.elsevier.com/locate/cattod

The promotional effect of transition metals on the catalytic behavior of model $Pd/Ce_{0.67}Zr_{0.33}O_2$ three-way catalyst

Guangfeng Li[a], Qiuyan Wang[a], Bo Zhao[a,b], Renxian Zhou[a,*]

[a] Institute of Catalysis, Zhejiang University, Xixi Campus, Hangzhou 310028, PR China
[b] School of Pharmaceutical and Chemical Engineering, Taizhou University, Taizhou 317000, PR China

ARTICLE INFO

Keywords:
$Ce_{0.67}Zr_{0.33}O_2$
Pd
Transition metals
TWCs
Catalytic activity

ABSTRACT

The behavior of Pd-only three-way catalysts supported on $Ce_{0.67}Zr_{0.33}O_2$ mixed oxides (CZ) doped by transition metals (M = Cr, Mn, Fe, Co, Ni) (Pd/CZM) have been examined under stoichiometric $CO + HC + NO_x + O_2$ reaction conditions and characterized. Different characterization techniques reveal that transition metal ions have entered into the ceria lattice and atomically more homogeneous mixed oxides have formed on the order of CZFe ≈ CZCo > CZNi ≈ CZ > CZMn > CZCr. It is confirmed that the homogeneity of ternary solid solution clearly modifies the properties of the samples and the catalytic behavior of the corresponding catalysts. The introduction of transition metals especially doped Fe and Co improves the oxygen mobility and strongly enhances the oxygen storage capacity of CZ and the corresponding catalysts. Moreover, the addition of Fe and Co into CZ forms more homogeneous Ce–Zr–M–O ternary solid solution and simultaneously promotes the reduction of CZ and Pd noble metal, respectively. It is worthwhile to note that it has a strong interaction between transition metals and Pd noble metal. Furthermore, the presence of Fe and Co obviously decreases the light-off temperature and significantly enhances the catalytic activity of the catalysts. Simultaneously, the windows of activity over Pd/CZFe and Pd/CZCo catalysts become wider compared to that of Pd/CZ.

1. Introduction

Three-way catalysts (TWCs) represent one of the most innovative technologies for automotive emission control. It can work simultaneously and efficiently to reduce NO and to oxidize CO and hydrocarbons (HC) in a narrow window of air/fuel ratio (A/F), close to the stoichiometric point [1–3]. Nevertheless, the increasingly strict limits imposed worldwide for automobile toxic emissions have forced consideration of new aspects and requirements in TWCs [4]. Extensive research and development has been performed for this purpose; for example, the performance of TWCs has been improved by the addition of many kinds of promoters. Although numerous investigations have been carried out to elucidate the effect of promoters, areas requiring study remain [2,5]. It is generally known that ceria–zirconia materials have earned much attention because of the ability of cerium to switch between the Ce^{4+} and Ce^{3+} oxidation states and to incorporate more or less oxygen into their crystal structure depending on various parameters, such as the gaseous atmosphere with which they are in contact, temperature and pressure [5–11]. Concerning the active metal components, the use of Pd as the only active metal in TWCs has received considerable attention on the basis of economic factors (i.e., the high cost and scarcity of Rh) and its remarkable activity for hydrocarbon and CO oxidation reactions [12]. However, the use of Pd in TWCs is restricted by the presence of lead in the fuel, which may strongly deactivate the noble metal by poisoning [13–16].

In recent years, typical TWCs formulations have included Pd as the active metal, fluorite-type oxides, such as ceria–zirconia, as promoters, and alumina as support, as well as other minor components, mainly present in order to enhance thermal stability and/or resistance to poisons [3,17,18]. The introduction of transition metals into ceria–zirconia [19–21] formed solid solutions, which promoted the redox property at lower temperature and achieved the lower light-off temperature during the cold start phase. This aspect has earned much attention in TWCs area [4,22–24], such as CeO_2–ZrO_2 doped with Mn [21], Cu [20,24], Fe and Ni [25]. Fernández-García et al. [19] studied the behavior of bimetallic $Pd–Cr/Al_2O_3$ and $Pd–Cr/(Ce,Zr)O_x/Al_2O_3$ catalysts for CO and NO elimination. The catalytic behavior of these bimetallic systems is strongly affected by the nature of the support and the interaction between the metal components. Hungría et al. [4,22,26] investigated the effect of Ni in $Pd–Ni/(Ce,Zr)O_x/Al_2O_3$ catalysts used for stoichiometric CO and NO elimination and revealed a significant dependence on the nature of the support in terms of the catalytic changes produced by nickel. Analysis of the $Pd–Ni/(Ce,Zr)O_x/Al_2O_3$ system shows the existence of preferential interactions of Pd and Ni

* Corresponding author. Tel.: +86 571 88273290; fax: +86 571 88273283.
E-mail address: zhourenxian@zju.edu.cn (R. Zhou).

0920-5861/$ – see front matter.
doi:10.1016/j.cattod.2010.05.001

with the (Ce,Zr)O_x and Al_2O_3 components, respectively. Lambrou et al. [27,28] studied the effects of Fe on the oxygen storage and release properties and the catalytic behavior of model Pd–Rh/CeO_2–Al_2O_3 three-way catalyst. The results indicate that iron (0.1–0.3 wt%) is deposited on both noble metals (Pd and Rh) and support, causing the development of electronic interactions that influences the oxidation states of Pd and Rh and enhances the oxygen chemisorption properties of ceria. The presence of Fe on the surface of the model TWCs also provides and/or creates new active catalytic sites for the reactions investigated. Thus, it could be concluded that Fe deposited on a commercial TWCs at least up to the level of 0.4 wt% acts likely as a promoter than a poison of its catalytic activity.

As mentioned above, a basic understanding of the interface effects between components may help to understand the chemicophysical phenomena associated with their structural and reduction properties as well as catalytic consequences [2,3,29]. More investigations on CeO_2–ZrO_2 doped with transition metals are required for understanding the real effect of the transition metals on the catalytic activity of Pd three-way catalysts.

In this study, a series of Pd-only three-way catalysts supported on CZ doped with transition metals (M = Cr, Mn, Fe, Co, Ni) have been prepared and characterized from a structural and textural point of view. In particular, we investigated the effects of introducing Cr, Mn, Fe, Co and Ni into CZ using a combination of X-ray diffraction (XRD), BET, high resolution transmission electron microscopy (HRTEM), oxygen storage capacity (OSC), Raman and H_2-temperature programmed reduction (H_2-TPR) and catalytic tests, focusing on the structural and oxygen storage capacity properties, reduction and catalytic activity behavior.

2. Experimental

2.1. Catalyst preparation

CZ doped with different transition metals (M referred to Cr, Mn, Fe, Co, Ni) was prepared through a co-precipitation route. The doping of transition metal was fixed at 5 wt%. $ZrO(NO_3)_2$, $Ce(NO_3)_3$ and $M(NO_3)_x{\cdot}nH_2O$ (referred to $Cr(NO_3)_3{\cdot}9H_2O$, $Mn(NO_3)_2$, $Fe(NO_3)_3{\cdot}9H_2O$, $Co(NO_3)_2{\cdot}6H_2O$, $Ni(NO_3)_2{\cdot}6H_2O$) were used as metal precursors. The required amounts of $ZrO(NO_3)_2$, $Ce(NO_3)_3$ and/or $M(NO_3)_x{\cdot}nH_2O$ were dissolved in water. The ammonia water was added dropwise to the solution of metal precursors to maintain the pH at about 9.5. The obtained slurry was aged at room temperature for 12 h, and then filtered, rinsed in deionized water and supercritically dried in ethanol medium (265 °C, 7.0 MPa) for 2 h. The samples were calcined at 500 °C in air for 4 h. All of the obtained supports were pressed into pellets, crushed and sieved to 40–60 meshes. The supports were designated CZ, CZCr, CZMn, CZFe, CZCo and CZNi, respectively.

M/CZ (designated Cr/CZ, Mn/CZ, Fe/CZ, Co/CZ, Ni/CZ) were prepared by incipient wetness impregnation method. 5% M/CZ support containing 5% of transition metal in weight was prepared by impregnation of the powder $Ce_{0.67}Zr_{0.33}O_2$ mixed oxides in aqueous solutions of $M(NO_3)_x{\cdot}nH_2O$ (referred to $Cr(NO_3)_3{\cdot}9H_2O$, $Mn(NO_3)_2$, $Fe(NO_3)_3{\cdot}9H_2O$, $Co(NO_3)_2{\cdot}6H_2O$, $Ni(NO_3)_2{\cdot}6H_2O$) overnight. The resulting sample was dried at 110 °C for 4 h and calcined at 500 °C in air for 4 h. All of the obtained supports were pressed into pellets, crushed and sieved to 40–60 meshes.

Eleven supported Pd catalysts with Pd content of 0.5 wt% (Pd/CZM designated Pd/CZ, Pd/CZCr, Pd/CZMn, Pd/CZFe, Pd/CZCo and Pd/CZNi; Pd/M/CZ designated Pd/Cr/CZ, Pd/Mn/CZ, Pd/Fe/CZ, Pd/Co/CZ and Pd/Ni/CZ) were also prepared by incipient wetness impregnation method, in which H_2PdCl_4 solution was used as Pd precursor. The resulting precipitate was reduced using hydrazine hydrate solution for 2 h, washed several times with water until without Cl^-, and then dried at 110 °C for 4 h followed by calcination at 500 °C for 2 h.

2.2. Catalytic activity measurement

Catalytic tests were carried out with a fixed-bed continuous flow reactor. A 0.2 ml catalyst sample was held in a quartz tube by packing quartz wool at both ends of the catalyst bed. The reaction mixture containing NO (0.1%)–NO_2 (0.03%)–C_3H_6 (0.067%)–C_3H_8 (0.033%)–CO (0.75%)–O_2 (0.745%) and balance Ar was fed to the reactor at a GHSV of 43,000 h^{-1}. The effluent gas was analyzed by on-line Fourier transform infrared spectrophotometer (BRUKER EQ55) equipped with a multiple reflection transmission cell (Infrared Analysis Inc.; path length 10.0 m). All spectra were taken at a resolution of 2 cm^{-1} for 128 scans. The air/fuel ratio experiments were carried out at 400 °C. The concentration of O_2 was adjusted in the tests of air/fuel ratio from 850 to 8440 ppm. The λ value of the simulated exhaust, which represents the ratio between the available oxygen and the oxygen needed for full conversion to CO_2, H_2O and N_2, is defined as $\lambda = \{2[O_2] + [NO] + 2[NO_2]\}/\{9[HC] + [CO]\}$, $\lambda = 1$ was at stoichiometry and the corresponding concentration of O_2 was 7450 ppm.

2.3. Characterization techniques

X-ray diffraction (XRD) measurement was performed on an ARL X'TRA X-ray Diffractometer (Thermo Electron Corporation, USA), with Cu Kα radiation, operating at 40 kV and 40 mA. Spectra were collected using a step size of 0.04° and a counting time of 5 s per angular abscissa in the range of 20–80° (2θ).

The textural properties were determined by N_2 adsorption using TriStarII3020 (Micromeritics Inc.). About 0.15 g of sample was degassed at 200 °C for 3 h under vacuum, and N_2 adsorption was carried out at −196 °C. Data were treated in accordance with the BET method. Surface morphology analysis was carried out using HRTEM on JEM-2010 apparatus operated at 200 kV. XEDS analysis was performed on an OXFORD INCA instrument attached to the transmission electron microscope to find out the chemical composition.

Raman spectra were recorded on a UV-HR Raman spectrograph with a He–Gd laser of 325 nm excitation wavelength. The samples were in powder form to prevent diffusion problems; spectra consisted of 2 accumulations of 30 s with a resolution of 4 cm^{-1}.

Hydrogen temperature programmed reduction (H_2-TPR) measurements were carried out to estimate the reducibility of the supports and catalysts. Each sample (50 mg) was pretreated at 300 °C for 30 min in air and cooled down to room temperature or −40 °C in N_2. The gas flow was then switched to 5% H_2/Ar, and the temperature was raised to 900 °C at a rate of 10 °C min^{-1}. The consumption of H_2 was monitored using a thermal conductivity detector (TCD).

Oxygen storage capacity measurement was carried out to estimate the total oxygen storage capacity (TOSC) using CHEMBET-3000 (Quantachrome Co.). A sample (100 mg) was reduced at 550 °C for 60 min in H_2 (10 ml/min), then cooled down to 200 °C and flushed with He (30 ml/min) for 20 min. 0.15 mL of O_2 was pulsed every 5 min until the intensity of the peak was a constant value.

3. Results and discussion

3.1. Textural and structural characterization

Fig. 1 shows the XRD patterns of the CZ doped by transition metals. The symmetrical peaks of the samples are consistent with the characteristic peaks of cubic fluorite-structured CeO_2, indicating the formation of Ce–Zr–M–O ternary solid solutions [7,30,3,32].

Table 1
Textural and structural properties of $Ce_{0.67}Zr_{0.33}O_2$ mixed oxides doped by transition metals.

Sample	Average pore diameter (nm)	S_{BET}(m^2/g)	Crystallite size (nm)	Lattice parameter (nm)
CZ	20.87	122.0	7.9	0.5407
CZCr	21.54	110.4	9.1	0.5389
CZMn	20.98	124.9	8.5	0.5377
CZFe	22.83	121.0	7.6	0.5336
CZCo	23.86	110.5	7.4	0.5356
CZNi	19.38	154.8	7.8	0.5386

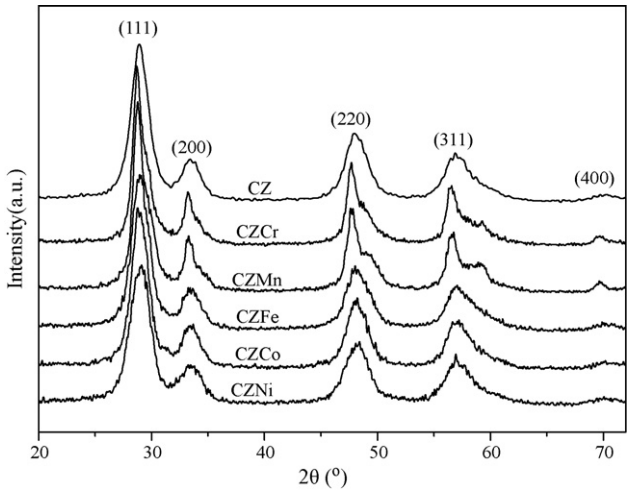

Fig. 1. XRD characterization of $Ce_{0.67}Zr_{0.33}O_2$ mixed oxides doped by transition metals.

And there is a little tetragonal t″ CZ crystal phase in the samples that is proved in Raman spectra (shown in Fig. 7). None of transition metals' diffraction peaks is observed in the XRD patterns of all samples, and this is mainly owing to the relatively high dispersion of such components or low loading of transition metals (5 wt%) below the detection limit of this technique. No splitting peaks related to pure CeO_2, ZrO_2 or transition metal phase can be observed, especially doped Fe and Co, which validates the homogeneity of Ce–Zr–M–O ternary solid solutions. With doping Cr and Mn, the diffraction peaks become sharper and the degree of symmetry becomes worse, indicating the growth of the nanocrystal or forming a non-homogeneous ternary solid solution.

Fig. 2 shows the HRTEM images of Pd/CZ, Pd/CZFe and Pd/CZCr catalysts. The pictures show the presence of nanoparticles of the CZ for three catalysts. Indeed, no Fe- or Cr-related particles could be identified in the multiple pictures, suggesting that all transition metal ions have entered into the Ce–Zr–M–O ternary solid solutions. Moreover, no Pd-related conglomerated particles could be identified in the multiple pictures taken for these catalysts, possibly due to the relatively high dispersion state of Pd noble metal in this system. Although the ionic radius of Cr^{3+} (0.64 Å) is smaller than that of Ce^{4+} (0.97 Å) and Zr^{4+} (0.84 Å), the average crystal size of the Pd/CZCr sample (Fig. 2c) increases compared to that of Pd/CZ. Combined with the XRD results and XEDS analysis of the Pd/CZCr catalyst, we estimate that conglomerated Cr ions are present on the lattice of Ce–Zr–Cr–O ternary solid solution.

Analyses of the cell parameter and particle size obtained from the XRD data as well as the BET surface area of the supports are summarized in Table 1. Since the ionic radius of transition metals is smaller than that of Ce^{4+} (0.97 Å) and Zr^{4+} (0.84 Å) for eight-coordination, the lattice constant of the cubic cell of Ce–Zr–M–O ternary solid solutions declines with doping transition metal ions into the mixed oxides. Therefore, we conclude that CZ doped with Fe and Co forms more homogeneous ternary solid solution, respectively, corresponding to the decrease of crystal size and lattice parameter. With doping Cr and Mn, the unit cell parameters calculated from the reflections of cubic ceria move from 0.5407 to 0.5389 and 0.5378 nm, respectively, but the crystal size increases compared to that of CZ. Combined with the HRTEM images of Pd/CZCr, we conclude again that conglomerated Cr or Mn ions exist in Ce–Zr–M–O ternary solid solution. It is reasonable to propose from the above discussions that transition metal ions have entered into the ceria lattice and more homogeneous mixed oxides have formed on the order of CZFe ≈ CZCo > CZNi ≈ CZ > CZMn > CZCr.

No clear relationship is observed between the BET surface area and the crystallite size of the samples calculated from the X-ray diffraction peaks, shown in Fig. 1. It is known that the introduction of Ni strongly enhances the surface area of CZ. When other transition metals are introduced, no clear promotional effects on the surface area of CZ are observed. It is worthwhile to note that the presence of Fe, Co within CZ obviously increases the average pore diameter of sample.

3.2. The reducibility of the samples

Fig. 3 shows H_2-TPR profiles of CZ doped by transition metals. For CZ, two reduction peaks appear in its TPR profile (referred to α, β), which may be ascribed to the reduction of subsurface and surface oxygen [11,33,34]. Obviously, α peak is shifted to lower temperature by the presence of transition metals, suggesting that the introduction of transition metals promotes the reduction of CZ. The reducibility of surface and subsurface oxygen of the samples is on the order of CZCo > CZFe > CZNi > CZMn > CZCr > CZ. Moreover,

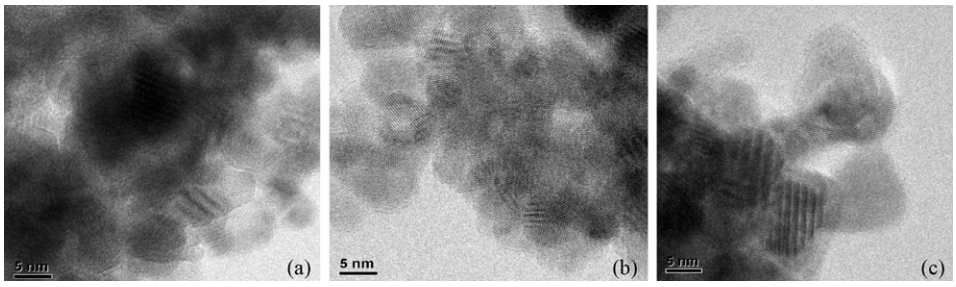

Fig. 2. HRTEM images of Pd/CZ (a), Pd/CZFe (b) and Pd/CZCr(c) catalysts.

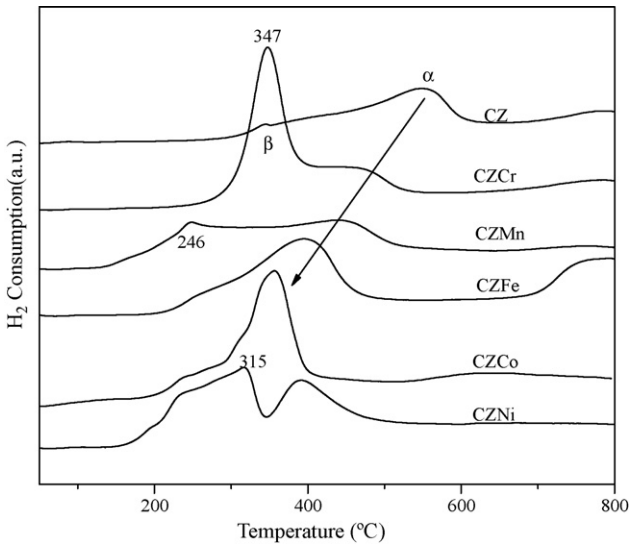

Fig. 3. H_2 consumption profiles during H_2-TPR over $Ce_{0.67}Zr_{0.33}O_2$ mixed oxides doped by transition metals.

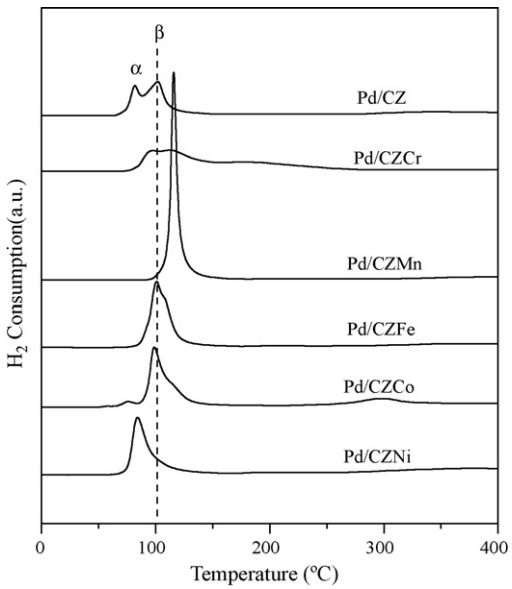

Fig. 4. H_2 consumption profiles during H_2-TPR over Pd/CZM catalysts.

only one stronger reduction peak appears at low temperature in the presence of Fe and Co, which promotes the reduction at low temperature and enhances oxygen mobility of the CZ. This is in accordance with Section 3.1 results that CZ doped with Fe and Co forms the homogeneous ternary solid solution, respectively. When Cr, Mn and Ni introduce into the CZ, the H_2 consumption profiles show two bands instead of a well-defined peak. The high temperature peak with low intensity is associated with the reduction of surface and subsurface oxygen of Ce–Zr–M–O solid solutions. The low temperature peak (referred to 347, 246 and 315 °C) can be attributed to the reduction of transition metal oxides (Cr_2O_3, MnO_2 and NiO) interacted with solid solution [24]. With Ce–Zr–Mn–O mixed oxides, the onset of Mn reduction at ca. 246 °C is lower than that of Mn in MnO_2, Mn_3O_4 and Mn_2O_3. This behavior can be attributed to the higher surface area in mixed oxides compared to that of pure MnO_x [24,35]. On the other hand, a certain degree of inhomogeneous distribution of solid solution also can be inferred. This is correlated well with the XRD results that conglomerated metal oxides exist in the solid solution with doping Cr and Mn.

Fig. 4 shows H_2-temperature programmed reduction profiles of Pd/CZM catalysts. Pd/CZ catalyst shows two maxima at ca. 81 and 101 °C, which can be associated with the reduction of PdO species highly dispersed on the surface of the support and formed on the interaction between PdO and the support [27,36], respectively. From Fig. 4, we can conclude that different catalysts have different reduction behavior. For Pd/CZFe and Pd/CZCo catalysts, only one stronger reduction peak appears at about 101 °C with a better symmetry, respectively. This behavior is attributable to the strong interaction between PdO and CZFe, CZCo, respectively. Based on the above results, we conclude that CZ doped with Fe and Co forms the homogeneous solid solution, respectively. Therefore, we propose that the presence of Fe and Co promotes the interaction between PdO and CZFe and/or CZCo, respectively. For Pd/CZNi catalyst, the reduction peak with high intensity appears at 81 °C, which can be associated to the reduction of PdO species highly dispersed on the surface of the support. We have known that the introduction of Ni strongly enhances the surface area of CZ. It suggests that the presence of Ni promotes the reduction of PdO species highly dispersed on the surface of the support. For Pd/CZCr and Pd/CZMn catalysts, the reduction peak of PdO species shifts to the higher temperature. This phenomenon may be correlated to the inhomogeneous of the support that make against the reduction of the PdO species.

M/CZ (designated as Cr/CZ, Mn/CZ, Fe/CZ, Co/CZ, Ni/CZ) supports were prepared by incipient wetness impregnation method. And the corresponding catalysts (Pd/M/CZ) were prepared. We investigated their reducibility of the supports and the catalytic activity of the catalysts. The H_2 consumption profiles during H_2-temperature programmed reduction over CZ impregnated by transition metals are shown in Figs. 5 and 6. For the supports (shown in Fig. 5), we can also conclude that α peak ascribed to the reduction of surface and subsurface oxygen is shifted to lower temperature by the presence of transition metals, suggesting that the introduction of transition metals promotes the reduction of CZ. Moreover, the low temperature peak (200–350 °C) attributed to the reduction of transition metal oxides appears in all supports, respectively. Furthermore, the intensity of the peak attributed to the reduction of transition metal oxides in Fig. 5 is higher than that of Fig. 3. Fig. 6 shows H_2-temperature programmed reduction profiles of Pd/M/CZ catalysts. The similar results are obtained in these profiles. For example, the reduction peak of PdO species shifts to the higher temperature

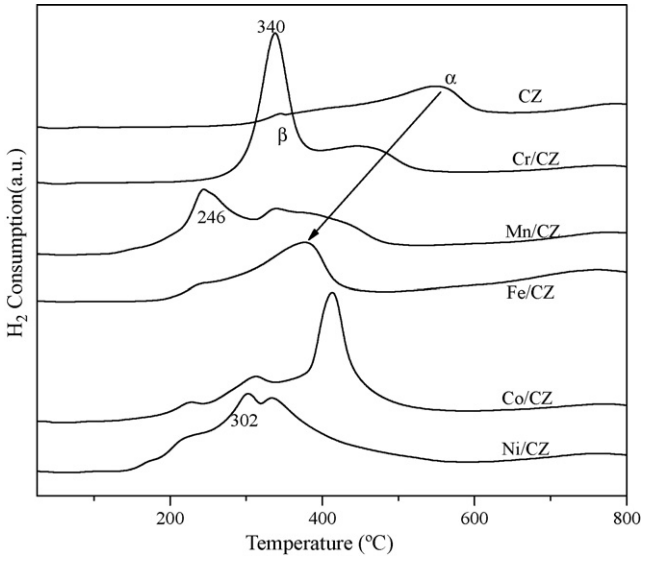

Fig. 5. H_2 consumption profiles during H_2-TPR over $Ce_{0.67}Zr_{0.33}O_2$ mixed oxides impregnated by transition metals.

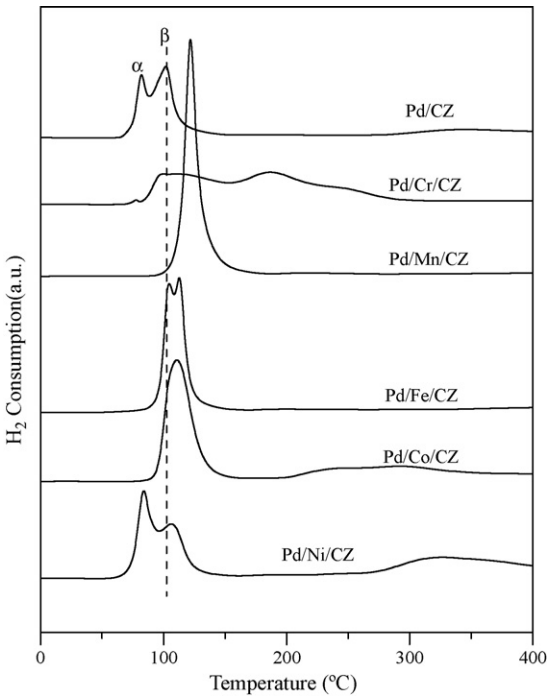

Fig. 6. H_2 consumption profiles during H_2-TPR over Pd/M/CZ catalysts.

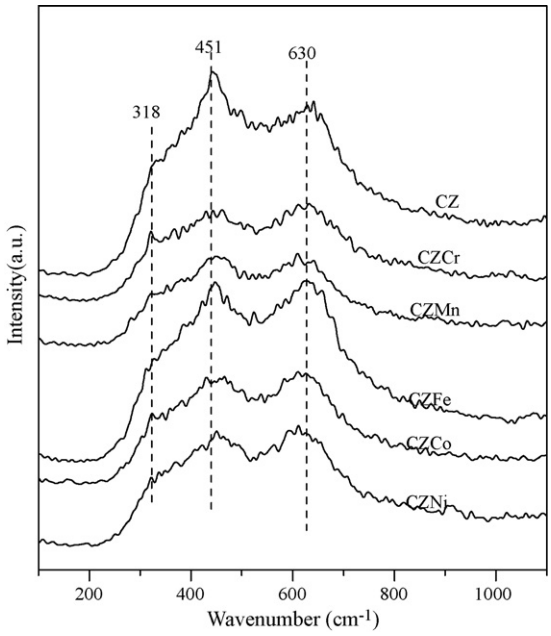

Fig. 7. Raman characterization of $Ce_{0.67}Zr_{0.33}O_2$ mixed oxides doped by transition metals.

over Pd/Cr/CZ and Pd/Mn/CZ catalysts. Moreover, the reduction peaks also shift to higher temperature over Pd/Fe/CZ, Pd/Co/CZ and Pd/Ni/CZ catalysts. Combined with Figs. 5 and 6, a certain degree of inhomogeneous distribution of solid solution prepared by impregnation also can be inferred. It can be speculated that the certain degree of homogeneous distribution of supports prepared by co-precipitation method is better than that prepared by impregnation method.

3.3. Oxygen storage capacity

Table 2 gives the oxygen storage capacity (OSC) of samples at 200 °C. From the table we can conclude that the presence of transition metals strongly enhances the oxygen storage capacity of supports and catalysts at lower temperature, respectively. It is confirmed that the oxygen storage capacity of the samples is on the order of CZFe > CZCo > CZNi > CZMn > CZCr > CZ. Moreover, the OSC of the catalyst is higher than that of corresponding support, respectively. In fact, OSC depends on both the nature of the metal and the support [37]. In that case, we have proved that CZ doped with Fe and Co forms the more homogeneous solid solution, and the radiuses of Fe and Co ions are smaller than that of Ce or Zr ions. Therefore, the presence of Fe and Co increases oxygen vacancy concentration and the oxygen storage capacity of the solid solution, respectively. On the contrary, CZ doped with Cr and Mn forms the inhomogeneous solid solution; the enhancement of OSC is less than that of CZFe or CZCo, respectively. It is worth pointing out that the improvement of OSC depends on the property of the solid solution and the oxygen environment.

Raman characterizations of CZ doped with transition metals (Cr, Mn, Fe, Co, Ni) are shown in Fig. 7. Two main bands at 451 and 630 cm^{-1} associated with the F_{2g} vibration of the fluorite-type lattice [11,38] and oxygen vacancies or lattice defects [38], respectively, are observed on all samples. Moreover, the A_{630}/A_{451} ratio reflecting the oxygen vacancy concentration increases with doping transition metals, especially for Fe and Co doping. It is also a sign of the improved oxygen mobility, which could be related to the presence of oxygen vacancies. The result is in accordance with the oxygen storage capacity of supports at 200 °C in Table 2.

The appearance of weak band at 318 cm^{-1} can be attributed to a tetragonal t″ CZ crystal phase, due to the displacement of oxygen atoms from their ideal fluorite lattice positions [30,39,40]. According to Yashima's study [41], in the so-called pseudo cubic structure t″, the cations remain to form a cubic structure, while the tetragonality is only presented by the O^{2-} displacement. Such a rearrangement of oxygen atoms means the transformation of cubic phase to a so-called pseudo cubic t″ phase, where cation sublattice remains cubic structure while oxygen atoms undergo a tetragonal distortion. The metastable t″ cannot be effectively detected by XRD technique due to weak diffraction ability of oxygen atoms, but be distinguished by the Raman spectroscopy thanks to its higher sensitivity to the oxygen displacements and smaller detection domain [31,42]. However, from the XRD patterns, we conclude that the doping of Fe and Co exhibits the better symmetry diffraction peaks, while with doping Cr and Mn, the diffraction peaks become sharper and the degree of symmetry becomes worse, possibly due to the presence of tetragonal t″ CZ crystal phase. From Fig. 7, it seems evident that the intensity of the peak at 318 cm^{-1} over supports is on the order of CZCr > CZMn > CZNi > CZ > CZCo > CZFe. Based on the discussion in Section 3.1, we have proposed that transition metal ions have entered into the ceria lattice and more homogeneous mixed oxides have formed atomically on the order of CZFe ≈ CZCo > CZNi ≈ CZ > CZMn > CZCr. Moreover, when doped Cr and Mn, the unit cell parameters calculated from the reflections

Table 2
Oxygen storage capacity of samples calculated as μmol O_2/g of sample at 200 °C.

Samples	CZ	CZCr	CZMn	CZFe	CZCo	CZNi
OSC(CZM)	358.8	477	487.5	617	558	514.8
OSC(Pd/CZM)	431.7	514.7	609.8	764.7	765.6	683

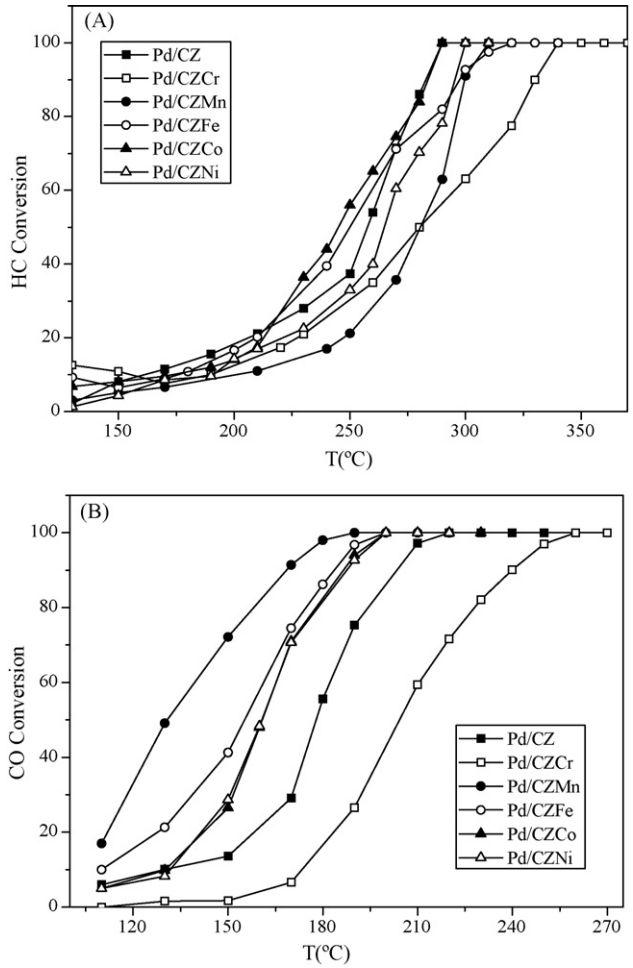

Fig. 8. Conversion of HC (A) and CO (B) as a function of reaction temperature under stoichiometric $CO + HC + NO_x + O_2$. Reaction condition: NO(0.1%)–NO_2(0.03%)–C_3H_6(0.067%)–C_3H_8(0.033%)–CO(0.75%)–O_2(0.745%) in Ar over various catalysts.

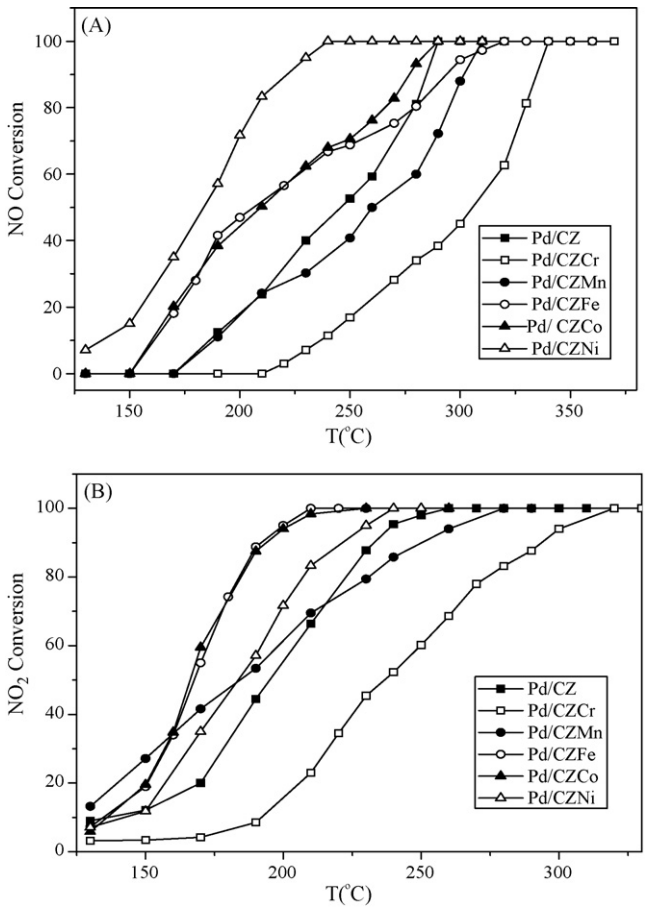

Fig. 9. Conversion of NO (A) and NO_2 (B) as a function of reaction temperature under stoichiometric $CO + HC + NO_x + O_2$. Reaction condition: NO(0.1%)–NO_2(0.03%)–C_3H_6(0.067%)–C_3H_8(0.033%)–CO(0.75%)–O_2(0.745%) in Ar over various catalysts.

of cubic ceria move from 0.5407 to 0.5389 and 0.5378 nm, respectively, but the crystal size increases compared to that of CZ. It may be due to the fact that conglomerated Cr ions are present on the lattice of Ce–Zr–Cr–O ternary solid solution. Combined with the intensity order of the peak at 318 cm^{-1} over supports, we speculate that the presence of tetragonal t″ phase also results in the inhomogeneity of solid solution.

3.4. Catalytic activity of the catalysts

The CO, HC, NO and NO_2 conversion as a function of temperature under stoichiometric $CO + HC + NO_x + O_2$ reaction over Pd/CZM catalysts are shown in Figs. 8 and 9. Among the catalysts tested here, Pd/CZFe and Pd/CZCo show the most activity, and Pd/CZCr the least. It seems that this behavior could be correlated well with above structural features of the supports. The homogeneous solid solution formed by CZ doped with Fe and Co strongly modifies the catalytic activity. On the contrary, the introduction of Cr forms the inhomogeneous ternary solid solution, and simultaneously a significant deactivation of the catalyst is observed. It suggests that the catalytic activity of the catalysts mainly depend on the property of the ternary solid solution. Table 3 summarizes the light-off temperature ($T_{50\%}$) and full-conversion temperature ($T_{90\%}$) of CO, HC, NO and NO_2 and the width of the window (W) over Pd/CZM catalysts. In our experiments, we also test the conversions of CO, HC and NO_x under different air/fuel ratios ($\lambda = 0.2$, 0.4, 0.6, 0.8, 1.0, 1.04, 1.07, 1.1, 1.15). The left side of the theoretical stoichiometric value ($\lambda = 1$) is lean oxygen, and the right is rich oxygen. W (λ value width) acts as another scale to evaluate catalyst property when CO, HC and NO_x conversions all reach

Table 3
Light-off temperature ($T_{50\%}$) and full-conversion temperature ($T_{90\%}$) of CO, HC, NO and NO_2 and the width of the window (W) over Pd/CZM catalysts.

Catalyst	$T_{50\%}$ (°C)				$T_{90\%}$ (°C)				W
	HC	CO	NO	NO_2	HC	CO	NO	NO_2	
Pd/CZ	258	178	246	195	283	204	284	233	0.221
Pd/CZCr	280	204	305	236	329	240	335	293	0.185
Pd/CZMn	280	131	260	184	300	168	301	250	0.220
Pd/CZFe	250	155	206	168	297	183	293	191	0.241
Pd/CZCo	245	161	210	167	283	186	276	193	0.253
Pd/CZNi	264	161	183	184	295	187	221	221	0.232

Table 4
Light-off temperature ($T_{50\%}$) and full-conversion temperature ($T_{90\%}$) of CO, HC, NO and NO_2 and the width of the window (W) over Pd/M/CZ catalysts.

Catalyst	$T_{50\%}$ (°C)				$T_{90\%}$ (°C)				W
	HC	CO	NO	NO_2	HC	CO	NO	NO_2	
Pd/CZ	258	178	246	195	283	204	284	233	0.221
Pd/Cr/CZ	276	230	322	254	341	275	345	310	0.167
Pd/Mn/CZ	262	106	260	158	309	154	301	236	0.217
Pd/Fe/CZ	262	159	198	167	309	190	299	188	0.223
Pd/Co/CZ	275	161	250	178	302	183	299	225	0.223
Pd/Ni/CZ	276	177	247	199	302	206	296	237	0.226

to 80% under rich and lean conditions. For example, the upper limit of the stoichiometric windows is limited by NO_x conversion under rich condition; the lower limit is limited by CO conversion under lean conditions for all samples. The upper limit subtracts the lower limit of λ is W value. Furthermore, the wider the W value is, the broader the three-way working window is. As can be seen from the table that the catalytic activity of the catalysts is on the order of Pd/CZFe ≈ Pd/CZCo > PdCZNi > PdCZ > Pd/CZMn > Pd/CZCr. This order is correlated well with that of atomically more homogeneous mixed oxides formed. The introduction of Fe and Co clearly decreases the light-off temperature of CO, HC, NO and NO_2 and enhances the catalytic activity of the catalysts, respectively. Moreover, the value of W increases, indicating that the window of activity becomes wider. Nevertheless, the presence of Ni and Mn decreases the light-off temperature of CO, NO and NO_2 and accelerates there full conversion. However, the introduction of Cr into CZ does not directly contribute to the catalytic performance instead restrain the catalytic activity. It indicates that the structure and properties of supports doped with transition metals are related to the catalytic activity of corresponding catalysts.

Table 4 summarizes the light-off temperature ($T_{50\%}$) and full-conversion temperature ($T_{90\%}$) of CO, HC, NO and NO_2 and the width of the window (W) over Pd/M/CZ catalysts. As also can be seen from the table that the property of solid solution impregnated with transition metals strongly influences the catalytic activity of the catalysts. The introduction of transition metals into CZ by impregnation forms the inhomogeneous solid solution; therefore, the activity of obtained catalysts is less than that in Table 3. Combined with Tables 3 and 4, we can conclude that the property of solid solution formed by introducing transition metals strongly influences the catalytic activity of the catalysts. Combined with H_2-TPR results, we can confirm again that the homogeneity of solid solution formed by doping transition metals strongly modifies the catalytic activity of the catalysts.

4. Conclusion

Through the above discussions, we have concluded that transition metal ions have entered into the ceria lattice and more homogeneous mixed oxides have formed on the order of CZFe ≈ CZCo > CZNi ≈ CZ > CZMn > CZCr. It is confirmed that this behavior can influence the properties of the supports and the catalytic activity of the catalysts. Among the catalysts tested here, Pd/CZFe and Pd/CZCo show the most activity, Pd/CZCr the least. Moreover, the presence of Fe and Co obviously decreases the light-off temperature and significantly enhances the catalytic activity of the catalysts. The catalytic activity of the catalysts is on the order of Pd/CZFe ≈ Pd/CZCo > PdCZNi > PdCZ > Pd/CZMn > Pd/CZCr. This order is correlated well with that of atomically more homogeneous mixed oxides formed.

Moreover, the H_2 consumption peaks are shifted to lower temperature by the presence of transition metals, suggesting that transition metals promote the reduction of supports. The reducibility of the supports is on the order of CZCo > CZFe > CZNi > CZMn > CZCr > CZ. And low temperature peaks are attributed to the reduction of transition metal oxides present on CZCr, CZMn and CZNi support, respectively. On the other hand, a certain degree of inhomogeneous distribution of solid solution also can be inferred. Among the Pd/CZM catalysts evaluated, the Pd/CZFe, Pd/CZCo and Pd/CZNi give a very sharp peak at the lower temperature, respectively, suggesting the quite fast reduction of Pd noble metal. It is worthwhile to note that it has a strong interaction between transition metals and Pd noble metal, promoting the catalytic activity of the catalysts. In all cases, the introduction of transition metals improves the oxygen mobility and strongly enhances the oxygen storage capacity of CZ, especially introduced into Fe and Co.

Acknowledgements

We gratefully acknowledge the financial supports from the Ministry of Science and Technology of China (Nos.: 2006AA060306 and 2009AA064804).

References

[1] X. Wu, J. Fan, R. Ran, J. Yang, D. Weng, J. Alloys Compd. 395 (2005) 135.
[2] M. Haneda, K. Shinoda, A. Nagane, O. Houshito, H. Takagi, Y. Nakahara, K. Hiroe, T. Fujitani, H. Hamada, J. Catal. 259 (2008) 223.
[3] A. Iglesias-Juez, A. Martínez-Arias, M. Fernández-García, J. Catal. 221 (2004) 148.
[4] A.B. Hungría, N.D. Browning, R.P. Erni, M. Fernández-García, J.C. Conesa, J.A. Pérez-Omil, A. Martínez-Arias, J. Catal. 235 (2005) 251.
[5] Y. Nagai, K. Dohmae, K. Teramura, T. Tanaka, G. Guilera, K. Kato, M. Nomura, H. Shinjoh, S. Matsumoto, Catal. Today 145 (2009) 279.
[6] R. Di Monte, J. Kašpar, H. Bradshaw, C. Norman, J. Rare Earths 26 (2) (2008) 136.
[7] D.M. Fernandes, A.A. Neto, M.J.B. Cardoso, F.M.Z. Zotin, Catal. Today 133–135 (2008) 574.
[8] M.V. Twigg, Appl. Catal. B 70 (2007) 2.
[9] J. Kašpar, P. Fornasiero, M. Graziani, Catal. Today 50 (1999) 285.
[10] A. Trovarelli, Catal. Sci. Series 2 (2002) 281.
[11] I. Atribak, A. Bueno-López, A. García-García, J. Catal. 259 (2008) 123.
[12] H. Zhu, J.R. Kim, S. Ki Ihm, Appl. Catal. B 86 (2009) 87.
[13] A. Martínez-Arias, M. Fernández-García, A.B. Hungría, A. Iglesias-Juez, K. Duncan, R. Smith, J.A. Anderson, J.C. Conesa, J. Soria, J. Catal. 204 (2001) 238.
[14] A. Martínez-Arias, A.B. Hungría, M. Fernández-García, A. Iglesias-Juez, J.A. Anderson, J.C. Conesa, J. Catal. 221 (2004) 85.
[15] M. Fernández-García, A. Iglesias-Juez, A. Martínez-Arias, A.B. Hungría, J.A. Anderson, J.C. Conesa, J. Soria, J. Catal. 221 (2004) 594.
[16] R. van Yperen, D. Lindner, L. Mubmann, E.S. Lox, T. Kreuzer, Stud. Surf. Sci. Catal. 116 (1998) 51.
[17] E.S.J. Lox, B.H. Engler, in: G. Ertl, H. Knözinger, J. Weitkamp (Eds.), Environ. Catal., Wiley–VCH, 1999, p. 1.
[18] A. Trovarelli, Catal. Rev. Sci. Eng. 38 (1996) 97.
[19] M. Fernández-García, A. Martínez-Arias, A. Iglesias-Juez, A.B. Hungría, J.A. Anderson, J.C. Conesa, J. Soria, J. Catal. 214 (2003) 220.
[20] X. Courtois, V. Perrichon, Appl. Catal. B 57 (2005) 63.
[21] L. Jia, M. Shen, J. Wang, X. Chu, J. Wang, Zh. Hu, J. Rare Earths 26 (2008) 523.
[22] A.B. Hungría, M. Fernández-García, J.A. Anderson, A. Martínez-Arias, J. Catal. 235 (2005) 262.
[23] A. Martínez-Arias, M. Fernaĭndez-Garcıĭa, A.B. Hungrıĭa, A. Iglesias-Juez, J.A. Anderson, Catal. Today 126 (2007) 90.
[24] D. Terribile, A. Trovarelli, C. de Leitenburg, A. Primavera, G. Dolcetti, Catal. Today 47 (1999) 133.
[25] V.R. Mastelaro, V. Briois, D.P.F. de Souza, C.L. Silva, J. Eur. Ceram. Soc. 23 (2003) 273.
[26] A.B. Hungría, J.J. Calvino, J.A. Anderson, A. Martínez-Arias, Appl. Catal. B 62 (2006) 359.

[27] P.S. Lambrou, A.M. Efstathiou, J. Catal. 240 (2006) 182.
[28] P.S. Lambrou, P.G. Savva, J.L.G. Fierro, A.M. Efstathiou, Appl. Catal. B 76 (2007) 375.
[29] P. Granger, C. Dujardin, J.-F. Paul, G. Leclercq, J. Mol. Catal. A 228 (2005) 241.
[30] J. Fan, X. Wu, X. Wu, Q. Liang, R. Ran, D. Weng, Appl. Catal. B 81 (2008) 38.
[31] X. Wu, X. Wu, Q. Liang, J. Fan, D. Weng, Zh. Xie, Sh. Wei, Solid State Sci. 9 (2007) 636.
[32] E. Aneggi, C. de Leitenburg, G. Dolcetti, A. Trovarelli, Catal. Today 114 (2006) 40.
[33] J. Wang, M. Shen, Y. An, J. Wang, Catal. Commun. 10 (2008) 103.
[34] M. Zhao, M. Shen, J. Wang, J. Catal. 248 (2007) 258.
[35] S. Imamura, M. Shono, N. Okamoto, A. Hamada, S. Ishida, Appl. Catal. A 142 (1996) 279.
[36] S. Zuo, R. Zhou, Micropor. Mesopor. Mater. 113 (2008) 472.
[37] C. Descorme, R. Taha, N. Mouaddib-Moral, D. Duprez, Appl. Catal. A 223 (2002) 287.
[38] C. Li, X. Gu, Y. Wang, Y. Wang, Y. Wang, X. Liu, G. Lu, J. Rare Earths 27 (2) (2009) 211.
[39] A. Iglesias-Juez, A.B. Hungría, A. Martínez-Arias, J.A. Anderson, M. Fernández-García, Catal. Today 143 (2009) 195.
[40] A. Martínez-Arias, M. Fernández-García, V. Ballesteros, L.N. Salamanca, C. Otero, J.C. Conesa, J. Soria, Langmuir 15 (1999) 4796.
[41] M. Yashima, H. Arashi, M. Kakihana, M. Yoshimura, J. Am. Ceram. Soc. 77 (1994) 1067.
[42] M. Yashima, K. Ohitake, M. Kakihana, H. Arashi, M. Yoshimura, J. Phys. Chem. Solids 57 (1996) 17.